

Preparation and Barrier Property of Poly(ethylene terephthalate)/Clay Nanocomposite Using Clay-Supported Catalyst

Won Joon Choi,¹ Hee-Joon Kim,² Kwan Han Yoon,¹ Oh Hyeong Kwon,¹ Chang Ik Hwang³

¹Department of Polymer Science and Engineering, Kumoh National Institute of Technology, Gumi, Gyeongbuk, South Korea

²Department of Applied Chemistry, Kumoh National Institute of Technology, Gumi, Gyeongbuk, South Korea

³R & D Center, Toray Seahan Inc., 287 Gongdan-Dong, Gumi, Gyeongbuk, South Korea

Received 27 April 2005; accepted 19 September 2005

DOI 10.1002/app.23268

Published online in Wiley InterScience (www.interscience.wiley.com).

ABSTRACT: Poly(ethylene terephthalate) (PET)/clay nanocomposite was prepared by the direct polymerization with clay-supported catalyst. The reaction degree of catalyst against the cation exchange capacity of clay was 8 wt %. The intercalation of PET chains into the silicate layers was revealed by X-ray diffraction studies. SEM morphology of the nanocomposite showed a good dispersion of clay-supported catalyst, ranging from 30 to 100 nm. The intercalated and

exfoliated clay-supported catalyst in PET matrix was also observed by TEM. The improvement of O₂ permeability for PET/clay-supported catalyst composite films over the pure PET is approximately factors of 11.3–15.6. © 2006 Wiley Periodicals, Inc. *J Appl Polym Sci* 100: 4875–4879, 2006

Key words: polyester; clay; nanocomposite film; clay-supported catalyst; barrier property

INTRODUCTION

Poly(ethylene terephthalate) (PET) has found a variety of application as fiber, bottles, films, and engineering plastics for automobiles and electronics because of its low cost and high performance. The primary objective of the development of PET/clay nanocomposites was to improve the gas barrier property that is required for beverage and food packagings.

One typical clay mineral, montmorillonite (MMT-Na), is composed of two silica tetrahedral sheets and alumina octahedral sheet, in which a part of Al³⁺ is replaced by Mg²⁺, generating negative charges within the clay layers. Their interlayers include exchangeable metal ions (e.g., Na⁺), neutralizing the net negative charges of the octahedral layers.¹

Recently, PET/clay nanocomposites have been reported and mainly focused on its synthesis,^{2–5} nanoscale morphology, and crystallization behavior.^{6,7} Qi and coworkers⁸ dispersed organically modified MMT in PET. Complete delamination was not achieved, but the tensile modulus of the nanocomposites increased as much as three times over that of pure PET. Tsai et al.⁹ reported that by using an amphoteric surfactant and an antimony acetate catalyst PET nanocomposites showed higher flexural strength and mod-

ulus than pure PET. Takagi and coworkers¹ reported that PET/clay hybrids exhibited favorable characteristics, such as improved tensile strength as well as optical transparency, by using ionic anchor monomer capable of being adsorbed onto clay surface.

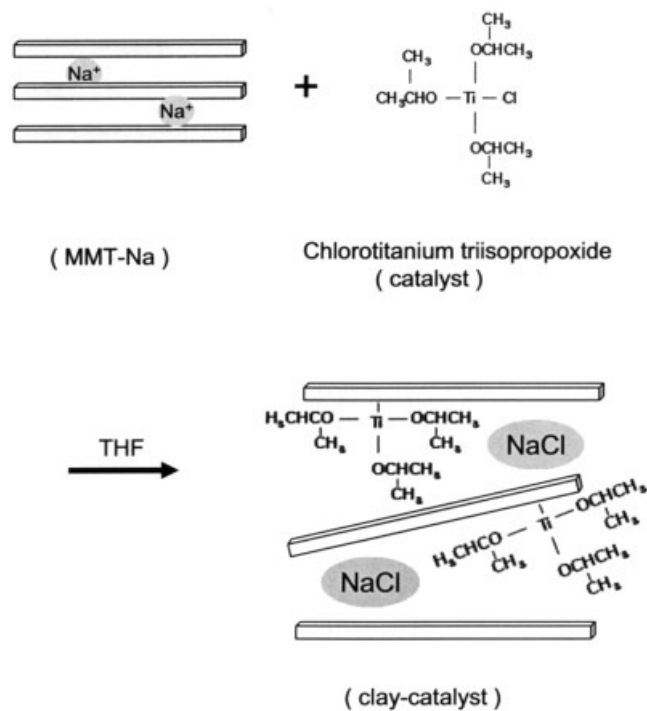
In this study, we tried to avoid a pre-existing intercalation method using organic compounds in which complete delamination was not achieved and brought in the thermal degradation^{10,11} during polymerization of PET due to the higher polymerization temperature. To overcome these disadvantages, we attempted to intercalate a catalyst directly into the clay interlayers by the metathesis reaction of the sodium cations with chlorotitanium catalyst. Morphology and wide-angle X-ray diffraction of composites as well as gas and moisture vapor transmission rate through the composite films were measured.

EXPERIMENTAL

Materials

Montmorillonite (MMT-Na) was purchased from Southern Clay, and the cation exchange capacity was 92.6 meq/100 g clay. Anhydrous tetrahydrofuran (THF) was purchased from Aldrich Chemical Co. Dimethyl terephthalate (DMT) and ethylene glycol (EG) were obtained from SK Chemical Co. and DaeJung Co., respectively. The catalyst used was chlorotitanium triisopropoxide.

Correspondence to: K. H. Yoon (khyoon@kumoh.ac.kr).



Scheme 1 Intercalation of catalyst into MMT interlayers.

Preparation of clay-supported catalyst

MMT was dried in a vacuum oven at 150°C for 24 h before use. In a 250-mL beaker, 10 g of MMT and 100 mL of anhydrous THF were mixed for 2 h at room temperature. Two grams of chlorotitanium triisopropoxide used as a catalyst was added to this suspension. The mixture was stirred for 24 h. A clay-supported catalyst was isolated by filtration and washed several times with anhydrous THF to remove unreacted catalyst. The reaction is shown in Scheme 1. The weight of clay-supported catalyst obtained was 10.8 g. It was estimated that the intercalation degree of catalyst against the cation exchange capacity was 8 wt %. This corresponds to 800 ppm of catalyst introduced in polymerization when PET/clay nanocomposite containing 1 wt % clay-supported catalyst is prepared.

Preparation of PET/clay-supported catalyst nanocomposite

PET/clay nanocomposites were prepared by melt polycondensation. In a small-scale batch reactor, 100 g of DMT, 64 g of EG, and 1 g of clay-supported catalyst were mixed. This mixture was first heated to 190°C in a silicone oil bath. This temperature was maintained for 2 h. The temperature was then increased to 210°C, where it was maintained for 2 h. The reaction temperature was progressively increased to 280°C. Then the pressure was reduced to a specified level and maintained for 0.5–1 h.

Measurements

The inherent viscosity of the composites was measured by using a mixed solvent of phenol/1,1,2,2-tetrachloroethane. The viscosity values ranged from 0.64 to 0.75 dL/g with the clay–catalyst content. The thermal stability of clay-supported catalyst was characterized under a nitrogen atmosphere at a heating rate of 10°C/min with a DuPont 910 thermogravimetric analyzer (TGA). Wide-angle X-ray diffraction measurements were performed on a Rigaku (D/Max-IIIB) X-ray diffractometer, using Ni-filtered Cu-K α radiation. The O₂ and moisture vapor transmission rate through PET and PET/clay-supported catalyst nanocomposite films were measured by using a MOCON 100. An average of three individual determinations was used.

RESULTS AND DISCUSSION

Thermal stability

To know the degradation of clay-supported catalyst during polymerization at 280°C, the thermal stability was measured. Figure 1 shows the TGA curves of catalyst, simple mixed catalyst plus MMT, clay, and clay-supported catalyst. The catalyst is easily degraded. For simple mixed catalyst plus MMT, the clay content remains after the degradation of catalyst. It is interesting to note that the clay-supported catalyst shows the less weight loss than the pure MMT at 100°C. The weight loss might be resulted from the chemisorbed waters. The weight loss of the pure MMT and clay-supported catalyst were 8 and 3 wt %, respectively, at 100°C. The difference in chemisorbed waters may result from the intercalation of the catalyst into the silicate layers. From the TGA results, it was

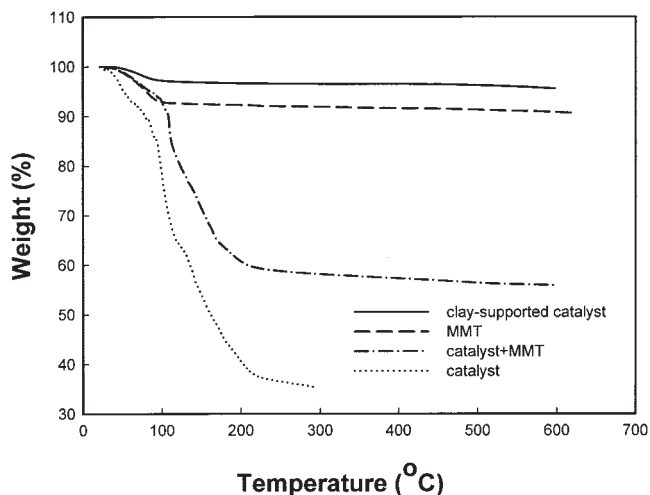


Figure 1 TGA curves of catalyst, simple mixed catalyst plus MMT, MMT and clay-supported catalyst.

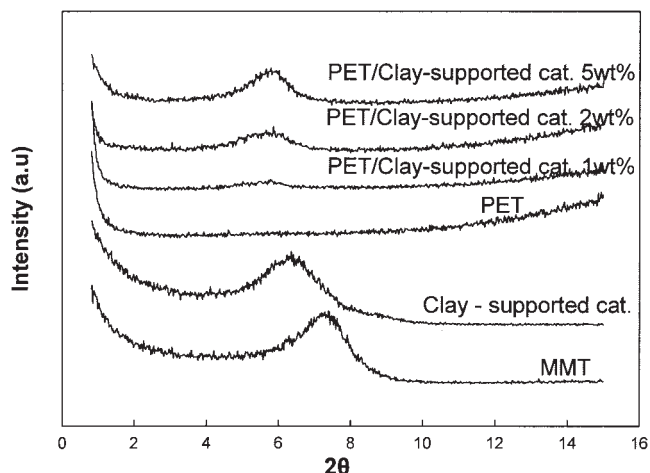


Figure 2 XRD patterns of MMT, clay-supported catalyst, and PET/clay nanocomposites.

confirmed that the thermal degradation of clay-supported catalyst during polymerization is not occurred.

Wide angle X-ray diffraction

Figure 2 shows X-ray diffraction results of the MMT, clay-supported catalyst, and PET/clay-supported catalyst nanocomposites. For the MMT, a peak occurs at $\sim 2\theta = 7.39^\circ$ ($d = 1.20$ nm). The peak of clay-supported catalyst is shifted to a lower angle, compared with that of MMT. This indicates that the interlayer spacing of the clay is increased. For PET/clay-supported catalyst nanocomposites, peak at $2\theta = 5.80^\circ$, corresponding to interlayer spacing of 1.52 nm, is clearly observed. This result implies that intercalation of PET chains into the galleries of silicate layers occurred, and exfoliation of the clay-supported catalyst in PET did not. As mentioned earlier, the intercalation degree of catalyst against the cation exchange capacity was 8 wt %, which indicates the most cations left. If it is considered that the intercalation of 8 wt % consists of real intercalation into the clay interlayer and the exchange reaction on the clay surface, the peak shift of PET/clay-supported catalyst nanocomposite to a lower angle was considerable.

Morphology

The importance of catalyst directly intercalated into the clay interlayer even though the small amount of catalyst was intercalated is shown in Figures 3 and 4. Figure 3 shows the morphology of PET/clay-supported catalyst nanocomposite containing 5 wt % of clay-supported catalyst, which was used as the highest amount in this study. The statistical results show that the particle sizes ranging from 30 to 100 nm. It can be seen that the particles are well dispersed. Figure 4

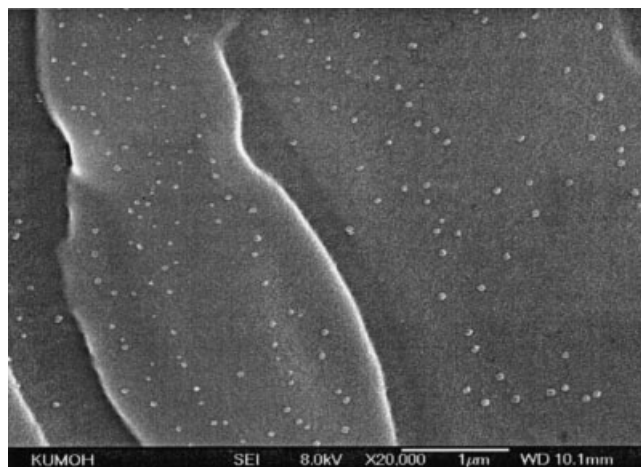


Figure 3 SEM morphology of PET/clay-supported catalyst nanocomposites containing 5 wt % of clay-supported catalyst.

shows the TEM photograph of 2 wt % nanocomposite. The light gray area is the PET matrix, and the darker regions are made up of silicate layers. It shows intercalated and exfoliated system. It indicates that the clay-supported catalyst was highly dispersed in the PET matrix, and some of the silicate layers are exfoliated into single layer (as shown in dotted circle) and randomly dispersed in PET matrix, although a number of unexfoliated layers still exist. From the SEM and TEM results, it was confirmed that a clay-supported catalyst plays an important role in exfoliation of silicate layers into PET matrix, although very small amount of intercalated clay-supported catalyst was used.

O₂ permeability

The reduction in gas permeability of PET depends on its crystallinity and filler loading levels. Hiltner and

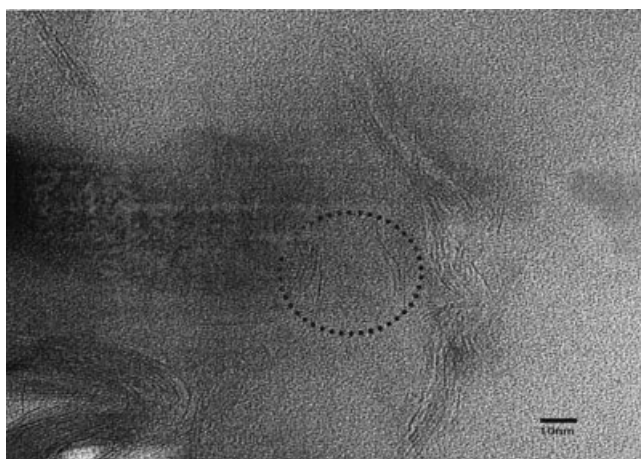


Figure 4 TEM photograph of PET/clay-supported catalyst nanocomposites containing 2 wt % of clay-supported catalyst.

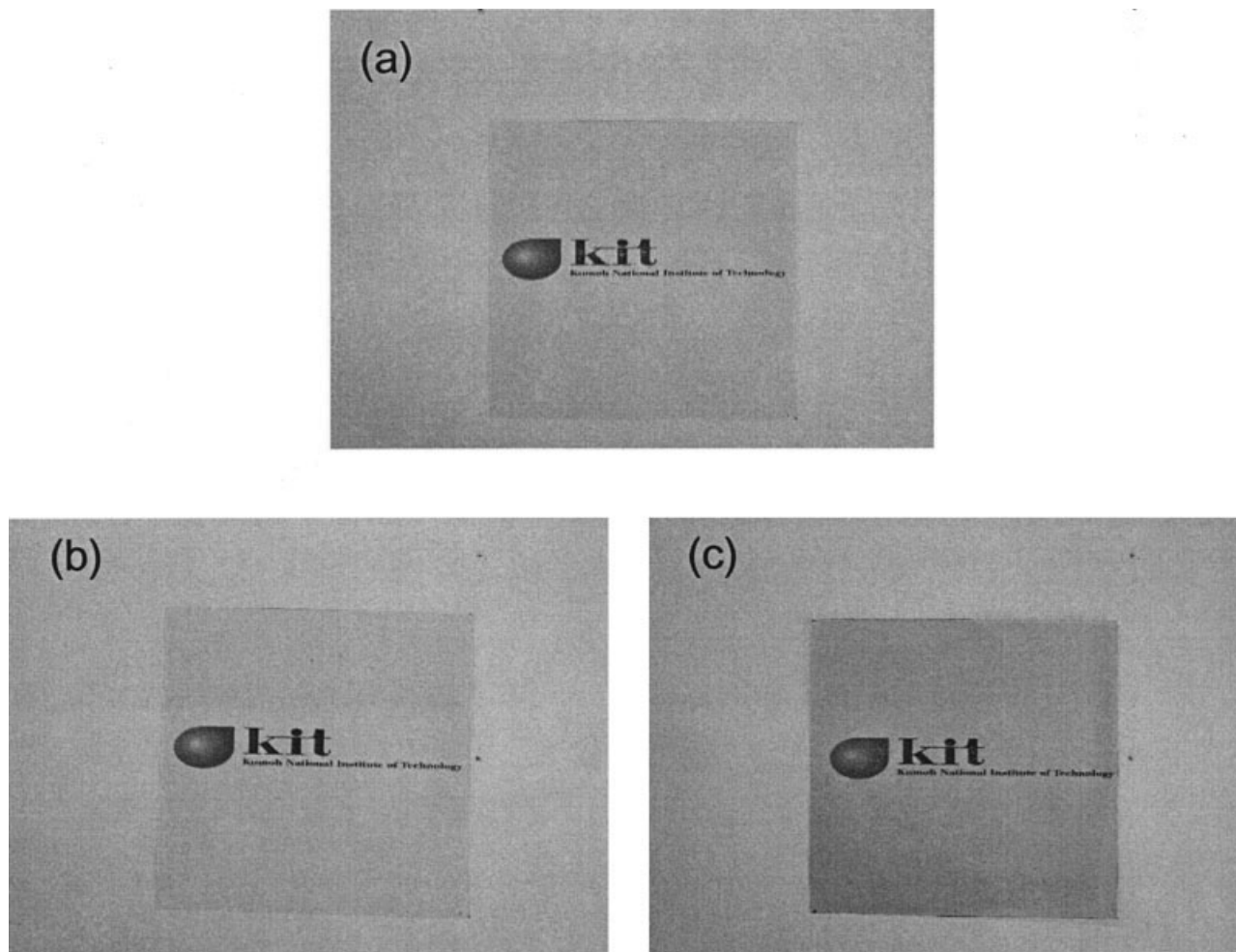


Figure 5 Transparency of the melted films of: (a) PET; (b) PET/clay-supported catalyst nanocomposite containing 2 wt % of clay-supported catalyst; and (c) PET/clay-supported catalyst nanocomposite containing 5 wt % of clay-supported catalyst.

coworkers^{12–16} have reported the relationship between the crystallinity and the oxygen permeability of PET, as well as the filler model, which follow a standard, predictable pattern, and dependent upon filler loading levels. In this study, to know the effect of only clay-supported catalyst, samples were quenched from the molten state and the crystallinity was not considered.

Figure 5 shows the photographs of PET and PET/clay-supported catalyst nanocomposite films, which are optically transparent, even though PET/clay-supported catalyst composite film containing 5 wt % reveals brown color.

The gas barrier properties have been shown to improve markedly upon exfoliation of clay platelets in a number of polymeric matrices.^{17–19} Bharadwaj et al.²⁰ reported the O₂ permeability for crosslinked polyester-clay nanocomposite. The improvement for the nanocomposite containing 2.5 wt % of clay was approximately a factor of 2.7. Gilmer et al.²¹ used the clay modified with a mixture of different ammonium ions. The improvement of O₂ permeability was a factor of 1.54. The mechanism for the improvement is

attributed to the increase in the tortuosity of the diffusive path for a penetrant molecule. The barrier properties through PET and PET/clay-supported catalyst composite films were measured and listed in Table I. As expected, the permeability of O₂ through the PET nanocomposite films was found considerably reduced

TABLE I
Barrier Properties of PET/Clay-Supported Catalyst Composite Films

Samples	Thickness (μm)	O ₂ TR ^a (cc/m ² /day)	MVTR ^b (g/m ² /day)
PET	170–180	857	22
PET/clay-supported catalyst (1 wt %)	170–190	76	26
PET/clay-supported catalyst (2 wt %)	160–170	61	21
PET/clay-supported catalyst (5 wt %)	160–170	55	19

^a Measured at 23°C and 0% relative humidity.

^b Measured at 38°C and 98% relative humidity.

with increasing clay-supported catalyst contents. The improvement of O₂ permeability for PET/clay-supported catalyst films over the pure PET is approximately factors of 11.3–15.6.

CONCLUSIONS

We presented here a new type clay-supported catalyst, unlike organoclay. Organoclay has two disadvantages: one is the lack of driving force into the silicate layers for PET polymerization, resulting in intercalated morphology; the other is the thermal degradation of organoclay during polymerization due to the higher polymerization temperature of PET. These disadvantages of organoclay can be overcome using the clay-supported catalyst. If a catalyst is intercalated in abundance into the silicate layers not on the surface, it is expected that fully exfoliated PET/clay-supported catalyst nanocomposite may be obtained, resulting in good barrier properties of PET composite film.

This research was supported by the Program for the Training of Graduate Students in Regional Innovation, which was conducted by the Ministry of Commerce, Industry and Energy of the Korean Government.

References

1. Zhang, G.; Shichi, T.; Takagi, K. *Mater Lett* 2003, 57, 1858.
2. Chang, J. H.; Kim, S. J.; Joo, Y. L.; Im, S. S. *Polymer* 2004, 45, 919.
3. Fu, X. A.; Qutubuddin, S. *Polym Eng Sci* 2004, 44, 345.
4. Ou, C. F.; Ho, M. T.; Lin, J. R. *J Appl Polym Sci* 2004, 91, 140.
5. Ke, Y. C.; Yang, X. B.; Zhu, C. F. *J Appl Polym Sci* 2002, 85, 2677.
6. Wang, Y.; Shen, C.; Li, H.; Li, Q.; Chen, J. *J Appl Polym Sci* 2004, 91, 308.
7. Wan, T.; Chen, L.; Chua, Y. C.; Lu, X. *J Appl Polym Sci* 2004, 94, 1381.
8. Ke, Y. C.; Long, C. F.; Qi, Z. N. *J Appl Polym Sci* 1999, 71, 1139.
9. Tasi, T. T.; Hwang, C. L.; Lee, S. Y. *SPE-ANTEC Proc* 2000, 248, 2412.
10. Saujanya, C.; Imai, Y.; Tateyama, H. *Polym Bull* 2002, 49, 69.
11. Davis, C. H.; Mathias, L. J.; Gilman, J. W.; Schiraldi, D. A.; Shields, J. R.; Trulove, P.; Sutto, T. E.; Delong, H. C. *J Polym Sci Part B: Polym Phys* 2002, 40, 2661.
12. Hu, Y. S.; Liu, R. Y. F.; Zhang, L. Q.; Rogunova, M.; Schiraldi, D. A.; Nazarenko, S.; Hiltner, A.; Baer, E. *Macromolecules* 2002, 35, 7326.
13. Hu, Y. S.; Schiraldi, D. A.; Hiltner, A.; Baer, E. *Macromolecules* 2003, 36, 3606.
14. Liu, R. Y. F.; Hu, Y. S.; Schiraldi, D. A.; Hiltner, A.; Baer, E. *J Appl Polym Sci* 2004, 94, 671.
15. Liu, R. Y. F.; Hu, Y. S.; Hibbs, M. R.; Collard, D. M.; Schiraldi, D. A.; Hiltner, A.; Baer, E. *J Appl Polym Sci* 2005, 98, 1615.
16. Hu, Y. S.; Hiltner, A.; Baer, E. *J Appl Polym Sci* 2005, 98, 1629.
17. Yano, K.; Usuki, A.; Okada, A.; Kuruuchi, T.; Kamigaito, O. *J Polym Sci Part A: Polym Chem* 1993, 31, 2493.
18. Yano, K.; Usuki, A.; Okada, A. *J Polym Sci Part A: Polym Chem* 1997, 35, 2289.
19. Lan, T.; Padmananda, D. K.; Pinnavaia, T. J. *Chem Mater* 1994, 6, 573.
20. Bharadwaj, R. K.; Mehrabi, A. R.; Hamilton, C.; Trujillo, C.; Murga, M.; Fan, R.; Chavira, A.; Thompson, A. K. *Polymer* 2002, 43, 3699.
21. Gilmer, J. W.; Barbee, R. B.; Matayabas, J. C., Jr.; Lan, T. U.S. Pat. 6,486,253 (2002).